

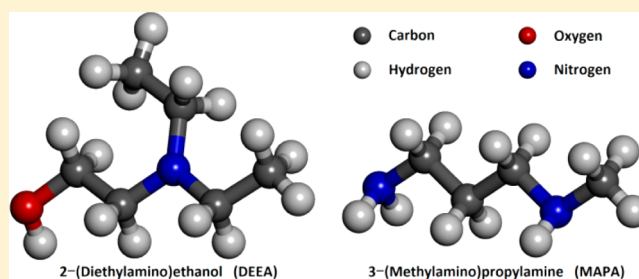
Equilibrium Total Pressure and CO₂ Solubility in Binary and Ternary Aqueous Solutions of 2-(Diethylamino)ethanol (DEEA) and 3-(Methylamino)propylamine (MAPA)

Muhammad Waseem Arshad,[†] Hallvard Fjøsne Svendsen,[‡] Philip Loldrup Fosbøl,[†] Nicolas von Solms,[†] and Kaj Thomsen^{*†}

[†]Department of Chemical and Biochemical Engineering, Center for Energy Resources Engineering (CERE), Technical University of Denmark (DTU), Søtofts Plads Building 229, DK-2800 Kongens Lyngby, Denmark

[‡]Department of Chemical Engineering, Norwegian University of Science and Technology (NTNU), NO-7491 Trondheim, Norway

ABSTRACT: Equilibrium total pressures were measured and equilibrium CO₂ partial pressures were calculated from the measured total pressure data in binary and ternary aqueous solutions of 2-(diethylamino)ethanol (DEEA) and 3-(methylamino)propylamine (MAPA). The measurements were carried out in a commercially available calorimeter used as an equilibrium cell. The examined systems were the binary aqueous solutions of 5 M DEEA, 2 M MAPA, and 1 M MAPA and the ternary aqueous mixtures of 5 M DEEA + 2 M MAPA (SD2M) and 5 M DEEA + 1 M MAPA (SD1M), which gave liquid–liquid phase split upon CO₂ absorption. The total pressures were measured and the CO₂ partial pressures were calculated as a function of CO₂ loading at three different temperatures 40 °C, 80 °C, and 120 °C. All experiments were reproduced with good repeatability. The measurements were carried out for 30 mass % MEA solutions to validate the experimental method. All the measured data were also compared with the results of 30 mass % MEA as a reference case. 5 M DEEA has shown high cyclic capacity. Both 2 M and 1 M MAPA showed high loading capacities at 40 °C and 120 °C. The aqueous amine mixtures, SD2M and SD1M, gave fairly good cyclic capacities and their results depend on the concentration of the promoter (MAPA) in the mixture. Approximate enthalpies of absorption of CO₂ in all the tested aqueous amine systems were estimated from the CO₂ solubility data. The measured total pressure and the estimated CO₂ solubility data can be useful in thermodynamic modeling of the capture systems when aqueous DEEA–MAPA solutions are used as capture solvents.



1. INTRODUCTION

Carbon dioxide (CO₂) is a well-known greenhouse gas and a major contributor to the global warming.¹ Fossil fuel based power generation is one of the major sources of CO₂ emissions worldwide.² The other large CO₂ emitting point sources are iron and steel industry, cement production plants, refineries, natural gas processing plants, and petrochemical production plants.³ Carbon capture and storage (CCS) is considered as a potential solution to reduce the CO₂ emissions and to mitigate the climate change.⁴ Among the available CCS technologies, the amine based absorption–desorption capture process is considered as the most mature technology due to its extensive use in different industrial application such as acid gas removal from natural gas.⁵ This technology can be retrofitted to the existing power generation plants, and the techno-economic feasibility studies indicate that the technology will remain competitive in the coming future.^{6,7} However, the major challenge with the amine scrubbing is the high energy requirements of the process.⁸ Technical improvements in the capture process and improved process design are one way to reduce the high energy demand of the process, the other being the design of energy efficient solvent systems.⁹

On the basis of the characteristics of different groups of amines, several amine-based solvent systems have been studied and reported in the literature. A few examples are (a) aqueous single alkanolamine solutions such as primary (monoethanolamine, MEA), secondary (diethanolamine, DEA), and tertiary (triethanolamine, TEA, and methyldiethanolamine, MDEA) alkanolamines,⁵ (b) aqueous amine blends (tertiary amine blended with primary or secondary amines as a promoter such as MEA + MDEA and DEA + MDEA)¹⁰ to exploit the favorable properties of different types of amines, and (c) sterically hindered amines¹¹ and cyclic amine (e.g., piperazine)¹² both as single aqueous solutions^{13–15} or as a blend of both together^{16–18} or a blend of each with other amines.^{19–21} One of the basic purposes of these and many other studies reported in the literature is to get the best solvent system with the characteristics of high CO₂ loading and cyclic capacity, fast reaction kinetics, low heat of absorption, low thermal and chemical degradation, low corrosion tendency, environmentally benign, and possibility of operating at elevated

Received: October 4, 2013

Accepted: January 7, 2014

Published: February 3, 2014

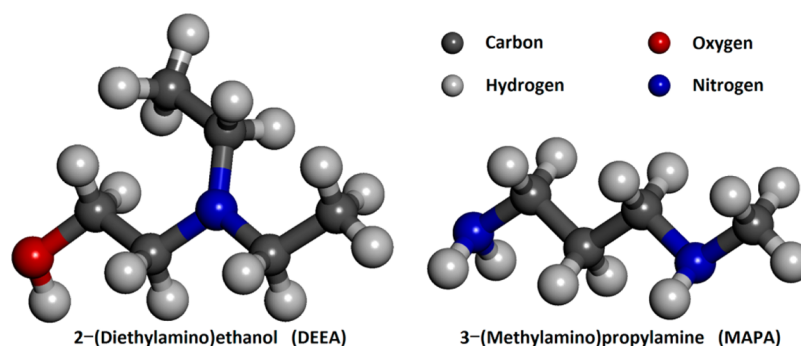


Figure 1. Molecular structures of DEEA (left) and MAPA (right).

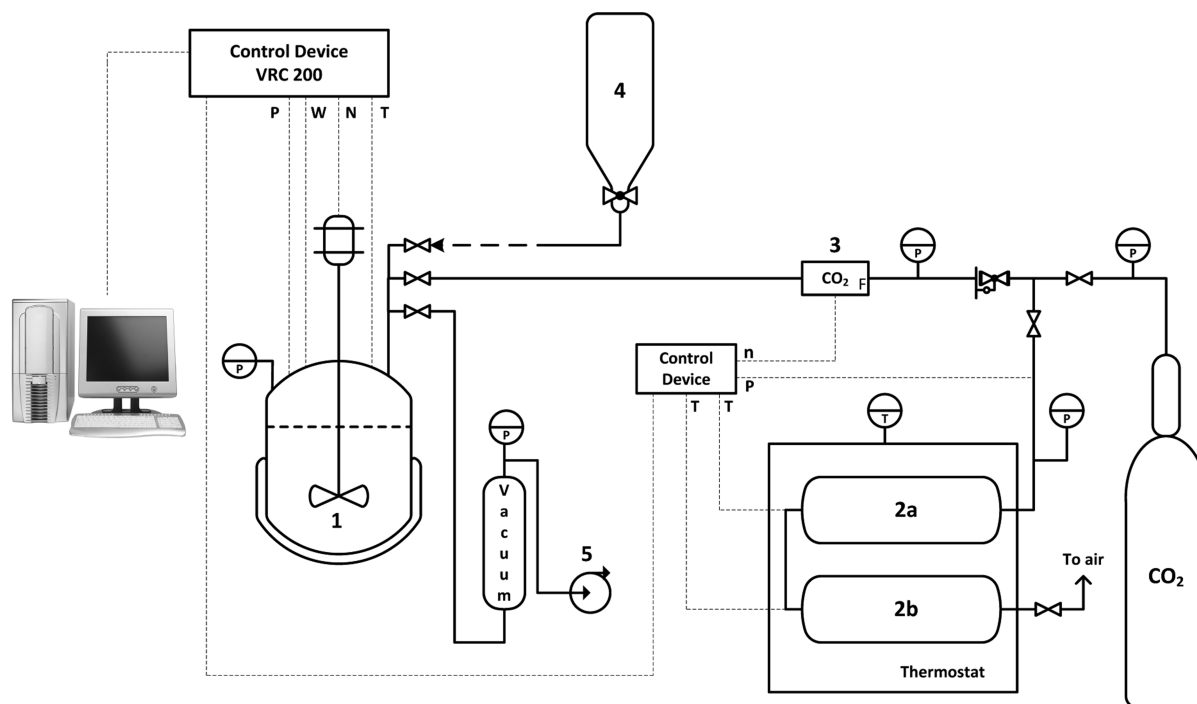


Figure 2. Schematic diagram of the experimental setup: 1, reaction calorimeter; 2a and 2b, CO₂ storage cylinders; 3, CO₂ mass flow controller; 4, amine solution feed bottle; 5, vacuum pump.

desorber pressures etc. High equilibrium temperature sensitivity is also advantageous which can reduce the stripping steam requirement in the desorber.²²

A new generation of mixed amine solvent systems, which can form two liquid phases, e.g., the thermomorphic biphasic solvents (TBS) systems²³ and the DMX process, has recently received attention.^{24,25} In the DMX process by IFPEN, the solvents form two immiscible phases after CO₂ absorption and only the CO₂ rich phase is sent to stripper for regeneration whereas the CO₂ lean phase is sent back to the absorber without regeneration. Due to low liquid circulation rate in the stripper, one can reduce the solvent regeneration energy. This process has claimed to reduce the reboiler duty down to 2.1 GJ·(ton CO₂)⁻¹ compared to 3.7 GJ·(ton CO₂)⁻¹ for the reference 30 mass % MEA process. On the other hand, the TBS systems absorb CO₂ and regenerate at a much lower temperature of 80 °C compared to the regeneration temperature of 120 °C for the conventional alkanolamine solutions. They give a liquid–liquid phase split during regeneration and become one liquid phase again during absorption. A lower solvent regeneration temperature is the main advantage of these systems, which can

be done without the use of steam.^{26,27} In this work a blend of amines, 2-(diethylamino)ethanol (DEEA) and 3-(methylamino)propylamine (MAPA), is under investigation. This system has the characteristics of biphasic liquid–liquid phase change solvents. MAPA is a diamine having a primary and a secondary amine functional group whereas DEEA is a tertiary alkanolamine. Molecular structures of both DEEA and MAPA are shown in Figure 1.

The equilibrium solubility data of CO₂ in aqueous amine solutions are essential for the design and modeling of the absorption–desorption capture processes. Such data are generally measured by using equilibrium cells. Extensive CO₂ solubility data are available in the literature for various amine systems measured with different equilibrium cells.^{28–32} These data are generally measured by using either static or dynamic (circulation) methods.³³ In the static method, an amine solution of known weight is taken in the equilibrium cell, CO₂ is injected, and the system is allowed to reach the equilibrium. When the equilibrium is established, the equilibrium pressure is recorded and compositions of the two phases (liquid and gas phases) are analyzed for CO₂ content. In the dynamic or circulation method, the amine solution is taken in the equilibrium cell followed by the

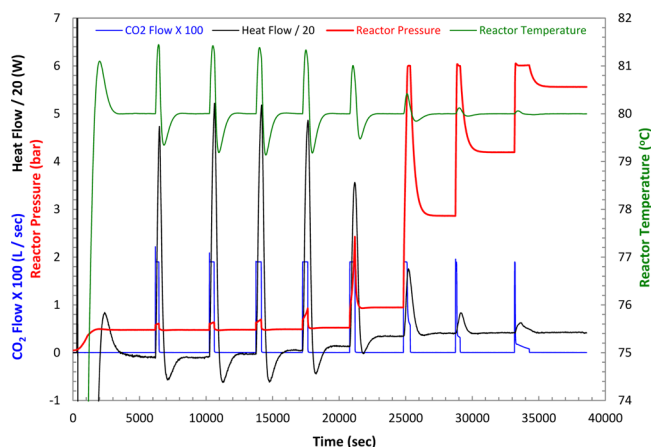


Figure 3. Example of different parameters (reactor temperature and pressure, heat flow, and CO₂ flow in the reactor) recorded as a function of time for one complete experiment of 1 M MAPA at 80 °C. To plot the multiple logged data on the left ordinate, CO₂ flow values were multiplied by 100 and heat flow values were divided by 20.

injection of nitrogen and the system is equilibrated at a preset temperature. The equilibrium pressure (nitrogen pressure + amine and water vapor pressure) is recorded and CO₂ is injected to the equilibrium cell. Then the vapor phase is circulated with the help of a circulating pump and the gas is bubbled through the liquid phase. When equilibrium is achieved, the total pressure of the system is recorded and the CO₂ partial pressure is calculated from the difference between the total pressure and the equilibrium pressure before introducing any CO₂ in the system.³³ Calorimeters have rarely been used for the solubility measurements. Xu and Rochelle presented total pressure measurements in aqueous amines at elevated temperatures by using the calorimeter and autoclave as the equilibrium cell.^{34,35} In the present work, the solubility measurements were carried out in a calorimeter that is generally used for the measurement of heat of absorption. The experimental method, in principle, resembles the static method with some differences. The advantage of using a calorimeter is the measurement of both CO₂ equilibrium solubility and heat of absorption in aqueous amine solutions at the same time. Our

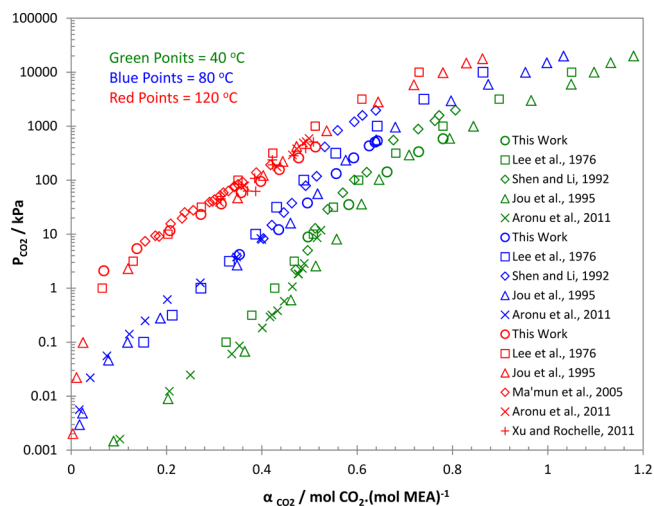


Figure 4. Comparison of partial pressure of CO₂ in 30 mass % MEA solutions as a function of CO₂ loading at 40 °C, 80 °C, and 120 °C from this work and the data from Lee et al.,²⁸ Shen and Li,²⁹ Jou et al.,³⁰ Ma'mun et al.,³¹ Aronu et al.,³² and Xu and Rochelle.³⁴

previous work presented the heat of absorption measurements in all the solvent systems studied in the present work.^{36,37}

The main objective of this work is the experimental measurements of equilibrium total pressure and estimation of CO₂ solubility from the measured total pressure data in aqueous solutions of DEEA, MAPA, and their mixtures. The selected concentration range of the aqueous amine mixtures gives a liquid–liquid phase split upon CO₂ absorption. Although some CO₂ solubility data were found in the literature for the binary aqueous DEEA solutions, there is a complete lack of CO₂ solubility data for the aqueous MAPA and mixed aqueous DEEA–MAPA systems. Another objective of this work is to validate the experimental method used for the measurements. For this, CO₂ solubility data were measured in 30 mass % MEA solutions and compared with the literature data. For all the amine systems studied in this work, the total pressure measurements were carried out by using the calorimeter as a function of amine composition, CO₂ loading, and the temperature ranging between 40 °C and 120 °C.

Table 1. Total Pressure and Solubility of CO₂ in 30 mass % MEA Solutions ($b_{\text{MEA}} = 7.017 \text{ mol MEA} \cdot (\text{kg H}_2\text{O})^{-1}$) at 40 °C, 80 °C, and 120 °C^a

α_{CO_2}	b_{CO_2}	P_{total}	P_{CO_2}	α_{CO_2}	b_{CO_2}	P_{total}	P_{CO_2}	α_{CO_2}	b_{CO_2}	P_{total}	P_{CO_2}
mol CO ₂ · (mol MEA) ⁻¹	mol CO ₂ · (kg H ₂ O) ⁻¹	kPa	kPa	mol CO ₂ · (mol MEA) ⁻¹	mol CO ₂ · (kg H ₂ O) ⁻¹	kPa	kPa	mol CO ₂ · (mol MEA) ⁻¹	mol CO ₂ · (kg H ₂ O) ⁻¹	kPa	kPa
313.15 K				353.15 K				393.15 K			
0.497	3.485	9.6	8.9	0.353	2.476	48.4	4.2	0.068	0.480	178.1	2.1
0.582	4.086	36.0	35.3	0.435	3.054	56.3	12.1	0.138	0.967	181.4	5.4
0.663	4.650	142.8	142.1	0.496	3.478	82.0	37.8	0.207	1.452	187.6	11.6
0.729	5.115	336.7	336.0	0.556	3.901	176.6	132.4	0.272	1.909	199.2	23.2
0.780	5.474	586.6	585.9	0.593	4.159	303.1	258.9	0.315	2.209	212.3	36.3
				0.625	4.387	477.0	432.8	0.357	2.502	234.7	58.7
				0.637	4.472	551.5	507.3	0.398	2.790	270.7	94.7
				0.642	4.506	579.5	535.3	0.437	3.063	332.8	156.8
								0.477	3.348	434.6	258.6
								0.512	3.595	587.2	411.2

^aThe standard uncertainty for the temperature is $u(T) = 0.03 \text{ K}$, and the relative standard uncertainties for the CO₂ composition are $u_r(b) = 0.01$ and $u_r(\alpha) = 0.01$. The estimated uncertainty for the measured P_{total} is $\pm 1\%$ for the total pressure below 50 kPa (with corresponding uncertainty of $\pm 2\%$ for the calculated P_{CO_2}), $\pm 0.7\%$ for P_{total} ranging between 51 kPa and 100 kPa (with corresponding uncertainty of $\pm 1.7\%$ for P_{CO_2}), and $\pm 0.5\%$ for P_{total} ranging between 101 kPa and 600 kPa (with corresponding uncertainty of $\pm 1.5\%$ for P_{CO_2}).

Table 2. Total Pressure and Solubility of CO₂ in 5 M (61.087 mass %) DEEA Solutions ($b_{\text{DEEA}} = 13.392 \text{ mol DEEA} \cdot (\text{kg H}_2\text{O})^{-1}$) at 40 °C, 80 °C, and 120 °C^a

α_{CO_2}	b_{CO_2}	P_{total}	P_{CO_2}	α_{CO_2}	b_{CO_2}	P_{total}	P_{CO_2}	α_{CO_2}	b_{CO_2}	P_{total}	P_{CO_2}
$\frac{\text{mol CO}_2}{(\text{mol DEEA})^{-1}}$	$\frac{\text{mol CO}_2}{(\text{kg H}_2\text{O})^{-1}}$	kPa	kPa	$\frac{\text{mol CO}_2}{(\text{mol DEEA})^{-1}}$	$\frac{\text{mol CO}_2}{(\text{kg H}_2\text{O})^{-1}}$	kPa	kPa	$\frac{\text{mol CO}_2}{(\text{mol DEEA})^{-1}}$	$\frac{\text{mol CO}_2}{(\text{kg H}_2\text{O})^{-1}}$	kPa	kPa
313.15 K (1)				353.15 K (1)				393.15 K (1)			
0.045	0.601	12.3	0.7	0.041	0.554	62.0	12.0	0.035	0.465	284.3	76.6
0.090	1.208	13.4	1.8	0.104	1.393	94.1	44.1	0.066	0.886	393.3	185.6
0.136	1.826	15.0	3.4	0.144	1.932	119.7	69.7	0.098	1.313	526.7	319.0
0.182	2.435	16.6	5.0	0.185	2.480	149.3	99.3	0.111	1.486	580.6	372.9
0.226	3.029	18.7	7.1	0.225	3.014	182.1	132.1	393.15 K (2)			
0.271	3.623	20.9	9.3	0.265	3.550	218.0	168.0	0.015	0.204	226.0	19.3
0.314	4.209	23.3	11.7	0.304	4.071	257.0	207.0	0.029	0.385	258.3	51.6
0.358	4.794	26.3	14.7	0.342	4.582	299.9	249.9	0.050	0.668	325.9	119.2
0.401	5.374	29.3	17.7	0.380	5.089	346.0	296.0	0.066	0.880	384.3	177.6
0.447	5.987	32.3	20.7	0.418	5.595	397.5	347.5	0.081	1.091	447.2	240.5
0.489	6.547	36.3	24.7	0.454	6.079	451.3	401.3	0.095	1.266	502.1	295.4
0.530	7.098	40.1	28.5	0.493	6.607	509.1	459.1	0.104	1.390	539.7	333.0
0.576	7.716	50.2	38.6	0.508	6.803	529.2	479.2	0.111	1.484	565.6	358.9
0.622	8.333	56.2	44.6	0.517	6.926	542.3	492.3	393.15 K (3)			
0.668	8.945	63.2	51.6	0.526	7.041	553.4	503.4	0.017	0.229	229.6	23.1
0.712	9.540	71.7	60.1	353.15 K (2)				0.032	0.430	271.3	64.8
0.755	10.112	82.2	70.6	0.038	0.510	60.7	10.6	0.050	0.670	332.7	126.2
0.798	10.691	97.0	85.4	0.077	1.035	78.1	28.0	0.069	0.926	407.2	200.7
0.840	11.246	119.6	108.0	0.134	1.793	111.3	61.2	0.088	1.175	490.2	283.7
0.880	11.783	155.1	143.5	0.189	2.529	151.2	101.1	0.100	1.339	545.0	338.5
0.918	12.289	218.1	206.5	0.243	3.256	197.6	147.5	0.107	1.436	575.6	369.1
0.954	12.773	330.5	318.9	0.296	3.969	249.8	199.7				
0.975	13.057	446.6	435.0	0.348	4.654	307.6	257.5				
0.987	13.213	527.7	516.1	0.398	5.326	370.5	320.4				
0.990	13.262	588.7	577.1	0.447	5.987	441.6	391.5				
313.15 K (2)				0.485	6.500	496.3	446.2				
0.039	0.527	12.0	0.6	0.502	6.720	519.9	469.8				
0.101	1.359	13.6	2.2	0.515	6.892	537.7	487.6				
0.164	2.201	15.8	4.4	0.525	7.024	550.4	500.3				
0.224	3.006	18.3	6.9								
0.284	3.805	21.2	9.8								
0.362	4.845	26.3	14.9								
0.438	5.868	32.0	20.6								
0.513	6.869	38.9	27.5								
0.598	8.004	47.6	36.2								
0.679	9.098	58.0	46.6								
0.759	10.170	72.7	61.3								
0.837	11.212	96.6	85.2								
0.893	11.961	130.5	119.1								
0.949	12.708	199.2	187.8								
0.983	13.162	287.5	276.1								
1.005	13.460	385.6	374.2								
1.020	13.653	469.7	458.3								
1.031	13.811	500.1	488.7								
1.038	13.902	549.9	538.5								

^aThe standard uncertainty for the temperature is $u(T) = 0.03 \text{ K}$, and the relative standard uncertainties for the CO₂ composition are $u_r(b) = 0.01$ and $u_r(\alpha) = 0.01$. The estimated uncertainty for the measured P_{total} is $\pm 1\%$ for the total pressure below 50 kPa (with corresponding uncertainty of $\pm 2\%$ for the calculated P_{CO_2}), $\pm 0.7\%$ for P_{total} ranging between 51 kPa and 100 kPa (with corresponding uncertainty of $\pm 1.7\%$ for P_{CO_2}), and $\pm 0.5\%$ for P_{total} ranging between 101 kPa and 600 kPa (with corresponding uncertainty of $\pm 1.5\%$ for P_{CO_2}).

2. EXPERIMENTAL SECTION

MEA (clear colorless liquid with a purity of ≥ 99 mass %), DEEA (clear pale yellow liquid with a purity of ≥ 99 mass %), and MAPA (clear colorless liquid with a purity of 99 mass %) were supplied by Sigma-Aldrich. Carbon dioxide (CO₂) with a purity of ≥ 99.99 mol % was purchased from AGA Gas GmbH.

All amines were used as received with no further purification. The amine sample solutions (mostly 2000 cm³ and a few cases with 1000 cm³) were prepared with deionized water by using an analytical balance (accuracy of ± 0.01 g) with standard uncertainty $u(x) = 0.00003$ mass fraction for the composition of the solutions.

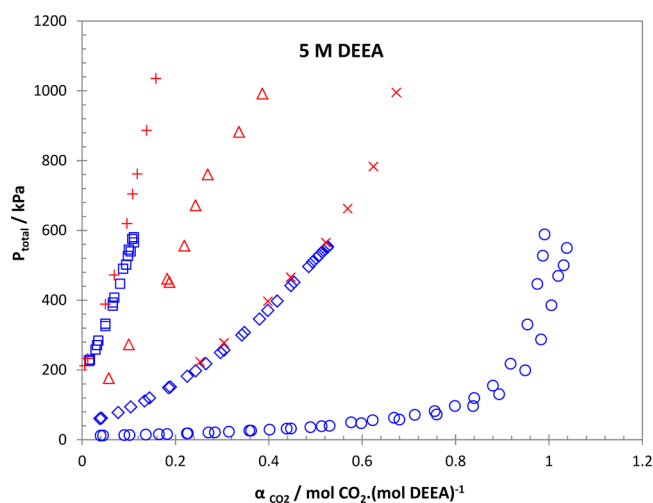


Figure 5. Comparison of total pressure in 5 M (~ 61.1 mass %) DEEA solutions as a function of CO₂ loading. This work (blue points): ○, 40 °C; ◇, 80 °C; □, 120 °C. Monteiro et al.³⁹ (red points): ×, 80 °C; △, 100 °C; +, 120 °C.

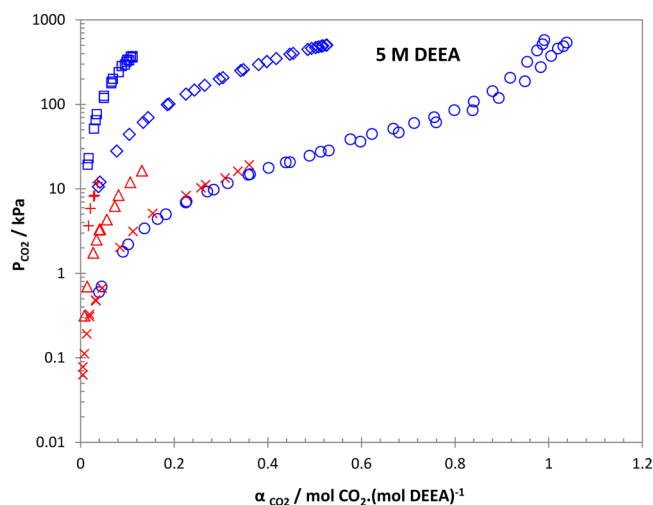


Figure 6. Comparison of partial pressure of CO₂ in 5 M (~ 61.1 mass %) DEEA solutions as a function of CO₂ loading. This work (blue points): ○, 40 °C; ◇, 80 °C; □, 120 °C. Monteiro et al.³⁹ (red points): ×, 40 °C; △, 60 °C; +, 80 °C.

A schematic diagram of the experimental setup is shown in Figure 2. The equipment details and the experimental method are similar to those described in the previous studies.^{37,38} Only the main features related to the total pressure measurements are highlighted here, which were not explained earlier.

The experimental setup consists of a thermally insulated jacketed reaction calorimeter (model CPA 122 from ChemiSens AB, Sweden), with a reactor volume of 2000 cm³, connected to two CO₂ storage cylinders (placed in a thermostatic water bath) through a precalibrated mass flow controller, amine solution feed bottle, and a vacuum pump. A data acquisition unit (VRC 200), connected to all the equipment and a computer, recorded all the operating parameters as a function of time.

Before feeding the amine sample solution into the reactor, it was evacuated and flushed with CO₂ to remove air and any inert gas present in the reactor. A known amount of amine solution (about 1200 cm³ to 1500 cm³) was then injected into the reactor and heated at a preset temperature to reach the equilibrium that was assured when the pressure and

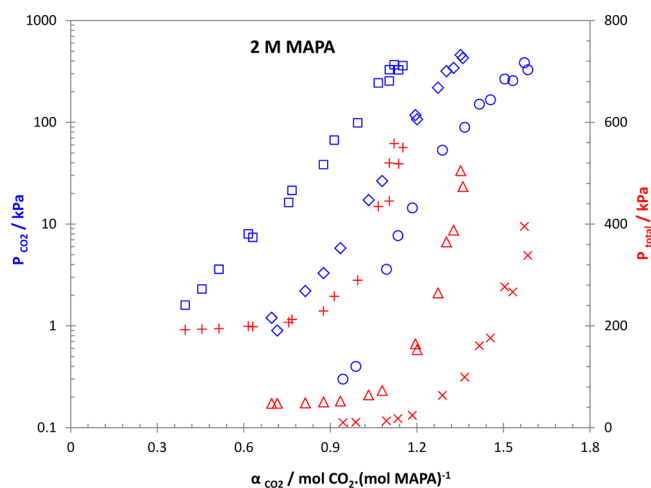


Figure 7. Total pressure and solubility of CO₂ in 2 M (~ 17.9 mass %) MAPA solutions as a function of CO₂ loading in this work. Total pressure (red points): ×, 40 °C; △, 80 °C; +, 120 °C. Partial pressure of CO₂ (blue points): ○, 40 °C; ◇, 80 °C; □, 120 °C.

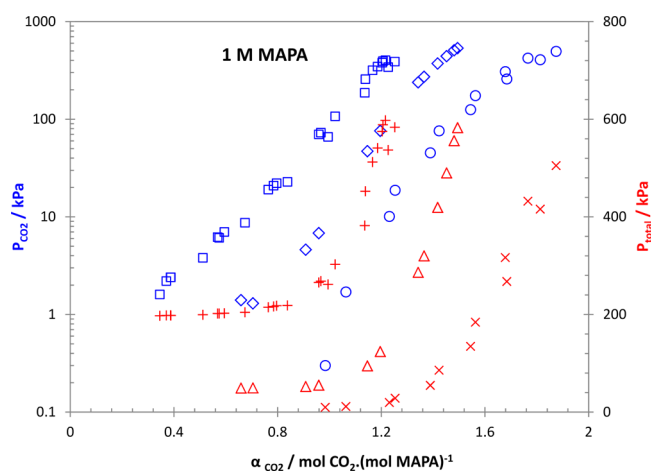


Figure 8. Total pressure and solubility of CO₂ in 1 M (~ 8.9 mass %) MAPA solutions as a function of CO₂ loading in this work. Total pressure (red points): ×, 40 °C; △, 80 °C; +, 120 °C. Partial pressure of CO₂ (blue points): ○, 40 °C; ◇, 80 °C; □, 120 °C.

temperature of the reactor changed within ± 0.01 bar and ± 0.01 °C. The equilibrium total pressure was recorded before injecting any CO₂ into the reactor. This total pressure before feeding any CO₂ into the reactor was the sum of partial pressures of amine and water vapors and represented as P_0 . Then a known small amount of CO₂ (0.1 mol to 0.3 mol) was fed to the reactor by recording the pressure difference in the CO₂ storage cylinders (the Peng–Robinson equation of state was used to calculate the amount of CO₂ fed to the reactor). The exothermic reaction between CO₂ and amine solution produced heat and the temperature increased inside the reactor, which was kept to isothermal conditions by the thermostatic jacket of the reactor. The system reached to a new equilibrium in 60 min to 90 min. The new equilibrium total pressure was also recorded, which is the sum of partial pressures of CO₂, amine, and water vapors, represented as P_t . The partial pressure of CO₂ (P_{CO_2}) was then calculated from the difference between the two total pressures as $P_{CO_2} = P_t - P_0$. CO₂ was continuously fed to the reactor until the amine solution was fully saturated. The corresponding CO₂ partial pressures were also calculated for each

Table 3. Total Pressure and Solubility of CO₂ in 2 M (17.877 mass %) MAPA Solutions ($b_{\text{MAPA}} = 2.469 \text{ mol MAPA} \cdot (\text{kg H}_2\text{O})^{-1}$) at 40 °C, 80 °C, and 120 °C^a

α_{CO_2}	b_{CO_2}	P_{total}	P_{CO_2}	α_{CO_2}	b_{CO_2}	P_{total}	P_{CO_2}	α_{CO_2}	b_{CO_2}	P_{total}	P_{CO_2}
$\text{mol CO}_2 \cdot (\text{mol MAPA})^{-1}$	$\text{mol CO}_2 \cdot (\text{kg H}_2\text{O})^{-1}$	kPa	kPa	$\text{mol CO}_2 \cdot (\text{mol MAPA})^{-1}$	$\text{mol CO}_2 \cdot (\text{kg H}_2\text{O})^{-1}$	kPa	kPa	$\text{mol CO}_2 \cdot (\text{mol MAPA})^{-1}$	$\text{mol CO}_2 \cdot (\text{kg H}_2\text{O})^{-1}$	kPa	kPa
313.15 K (1)				353.15 K (1)				393.15 K (1)			
0.943	2.330	10.1	0.3	0.696	1.720	47.7	1.2	0.397	0.979	192.4	1.6
1.094	2.703	13.4	3.6	0.813	2.008	48.7	2.2	0.514	1.269	194.4	3.6
1.184	2.924	24.2	14.4	0.935	2.308	52.3	5.8	0.631	1.558	198.2	7.4
1.365	3.372	99.2	89.4	1.079	2.666	73.0	26.5	0.755	1.866	207.1	16.3
1.455	3.593	176.3	166.5	1.200	2.964	153.4	106.9	0.876	2.163	229.2	38.4
1.532	3.784	266.6	256.8	1.273	3.144	264.9	218.4	0.995	2.457	289.6	98.8
1.584	3.912	338.3	328.5	1.327	3.277	388.1	341.6	1.104	2.726	445.2	254.4
313.15 K (2)				353.15 K (2)				393.15 K (2)			
0.988	2.440	10.6	0.4	0.716	1.768	48.1	0.9	1.137	2.807	518.4	327.6
1.134	2.801	17.9	7.7	0.876	2.164	50.5	3.3	1.151	2.843	550.5	359.7
1.288	3.181	63.4	53.2	1.033	2.550	64.4	17.2	1.121	2.768	558.2	367.0
1.416	3.497	160.9	150.7	1.195	2.951	164.6	117.4	1.104	2.727	520.0	328.8
1.504	3.715	276.6	266.4	1.302	3.215	364.9	317.7	1.121	2.768	558.2	367.0
1.572	3.883	395.3	385.1	1.351	3.337	504.9	457.7				

^aThe standard uncertainty for the temperature is $u(T) = 0.03 \text{ K}$, and the relative standard uncertainties for the CO₂ composition are $u_r(b) = 0.01$ and $u_r(\alpha) = 0.01$. The estimated uncertainty for the measured P_{total} is $\pm 1\%$ for the total pressure below 50 kPa (with corresponding uncertainty of $\pm 2\%$ for the calculated P_{CO_2}), $\pm 0.7\%$ for P_{total} ranging between 51 kPa and 100 kPa (with corresponding uncertainty of $\pm 1.7\%$ for P_{CO_2}), and $\pm 0.5\%$ for P_{total} ranging between 101 kPa and 600 kPa (with corresponding uncertainty of $\pm 1.5\%$ for P_{CO_2}).

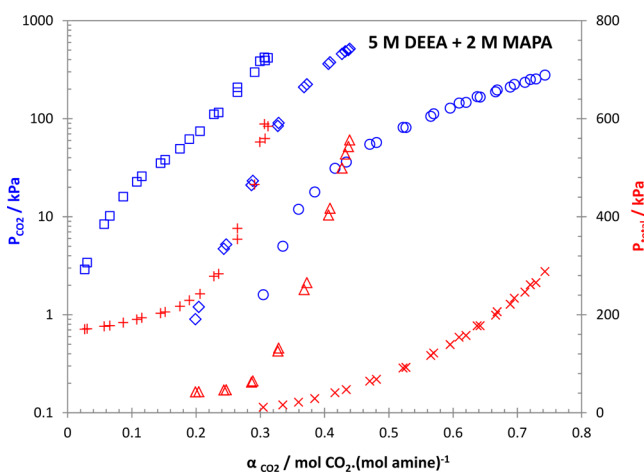


Figure 9. Total pressure and solubility of CO₂ in 5 M (~ 63.5 mass %) DEEA + 2 M (~ 19.1 mass %) MAPA solutions as a function of CO₂ loading in this work. Total pressure (red points): ×, 40 °C; △, 80 °C; +, 120 °C. Partial pressure of CO₂ (blue points): ○, 40 °C; ◇, 80 °C; □, 120 °C.

CO₂ feeding cycle by assuming that the P_0 remained constant throughout the experiment. All the necessary operating parameters were logged against time. An example of logged data for one complete experiment of 1 M MAPA at 80 °C is shown in Figure 3. The blue line indicates the injection of CO₂ into the reactor (eight times) and the black, green, and red lines, respectively, represent the corresponding heat flow, reactor temperature, and reactor pressure. The equilibrium total pressure in the reactor increased up to approximately 6 bar at the end of the experiment. The measurements were made isothermally at 40 °C, 80 °C, and 120 °C for all the systems studied in this work. The measured equilibrium total pressure and the calculated CO₂ partial pressure data are presented as a function of CO₂ loading.

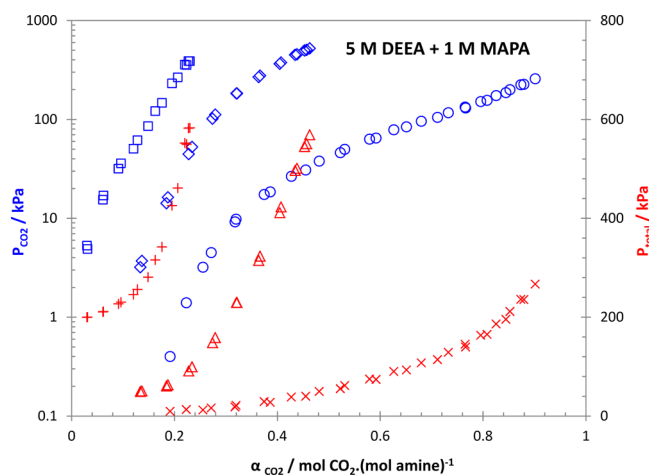


Figure 10. Total pressure and solubility of CO₂ in 5 M (~ 62 mass %) DEEA + 1 M (~ 9.3 mass %) MAPA solutions as a function of CO₂ loading in this work. Total pressure (red points): ×, 40 °C; △, 80 °C; +, 120 °C. Partial pressure of CO₂ (blue points): ○, 40 °C; ◇, 80 °C; □, 120 °C.

The total pressure data were measured with an estimated uncertainty of $\pm 1\%$ for P_{total} below 50 kPa (with corresponding uncertainty of $\pm 2\%$ for the calculated P_{CO_2} from the total pressure data), $\pm 0.7\%$ for P_{total} ranging between 51 kPa and 100 kPa (with corresponding uncertainty of $\pm 1.7\%$ for P_{CO_2}), and $\pm 0.5\%$ for P_{total} ranging between 101 kPa and 600 kPa (with corresponding uncertainty of $\pm 1.5\%$ for P_{CO_2}).

3. RESULTS AND DISCUSSION

Equilibrium total pressures were measured and CO₂ partial pressures were estimated from the total pressure measurements in binary and ternary aqueous solutions of DEEA and MAPA

Table 4. Total Pressure and Solubility of CO₂ in 1 M (8.901 mass %) MAPA Solutions ($b_{\text{MAPA}} = 1.108 \text{ mol MAPA} \cdot (\text{kg H}_2\text{O})^{-1}$) at 40 °C, 80 °C, and 120 °C^a

α_{CO_2}	b_{CO_2}	P_{total}	P_{CO_2}	α_{CO_2}	b_{CO_2}	P_{total}	P_{CO_2}	α_{CO_2}	b_{CO_2}	P_{total}	P_{CO_2}
$\frac{\text{mol CO}_2}{(\text{mol MAPA})^{-1}}$	$\frac{\text{mol CO}_2}{(\text{kg H}_2\text{O})^{-1}}$	kPa	kPa	$\frac{\text{mol CO}_2}{(\text{mol MAPA})^{-1}}$	$\frac{\text{mol CO}_2}{(\text{kg H}_2\text{O})^{-1}}$	kPa	kPa	$\frac{\text{mol CO}_2}{(\text{mol MAPA})^{-1}}$	$\frac{\text{mol CO}_2}{(\text{kg H}_2\text{O})^{-1}}$	kPa	kPa
313.15 K (1)				353.15 K (1)				393.15 K (1)			
0.984	1.091	9.7	0.3	0.705	0.781	49.5	1.3	0.345	0.383	197.2	1.6
1.231	1.364	19.5	10.1	0.959	1.063	55.0	6.8	0.512	0.567	199.4	3.8
1.389	1.540	54.6	45.2	1.196	1.326	124.1	75.9	0.674	0.747	204.3	8.7
1.544	1.712	134.6	125.2	1.365	1.513	320.0	271.8	0.838	0.929	218.4	22.8
1.684	1.867	267.6	258.2	1.452	1.610	490.0	441.8	0.995	1.103	261.5	65.9
1.813	2.010	415.6	406.2	1.495	1.657	582.7	534.5	1.136	1.260	382.1	186.5
1.875	2.078	505.0	495.6	353.15 K (2)				1.227	1.360	536.9	341.3
313.15 K (2)				0.659	0.730	49.1	1.4	1.252	1.388	583.6	388.0
1.063	1.179	11.4	1.7	0.908	1.007	52.3	4.6	393.15 K (2)			
1.253	1.389	28.4	18.7	1.146	1.271	94.7	47.0	0.387	0.429	198.1	2.4
1.423	1.577	85.7	76.0	1.342	1.488	286.3	238.6	0.574	0.637	201.8	6.1
1.563	1.732	184.1	174.4	1.418	1.571	419.4	371.7	0.796	0.883	217.8	22.1
1.678	1.860	316.6	306.9	1.481	1.642	556.1	508.4	1.022	1.133	302.6	106.9
1.766	1.957	432.2	422.5					1.186	1.315	540.9	345.2
								1.216	1.348	597.8	402.1
								393.15 K (3)			
								0.370	0.411	197.9	2.2
								0.569	0.630	201.9	6.2
								0.764	0.847	214.7	19.0
								0.959	1.063	265.5	69.8
								1.139	1.262	452.3	256.6
								1.204	1.334	575.0	379.3
								393.15 K (4)			
								0.388	0.430	197.8	2.4
								0.594	0.659	202.4	7.0
								0.785	0.870	216.3	20.9
								0.967	1.072	268.2	72.8
								1.166	1.293	512.2	316.8
								1.206	1.337	588.6	393.2

^aThe standard uncertainty for the temperature is $u(T) = 0.03 \text{ K}$, and the relative standard uncertainties for the CO₂ composition are $u_r(b) = 0.01$ and $u_r(\alpha) = 0.01$. The estimated uncertainty for the measured P_{total} is $\pm 1\%$ for the total pressure below 50 kPa (with corresponding uncertainty of $\pm 2\%$ for the calculated P_{CO_2}), $\pm 0.7\%$ for P_{total} ranging between 51 kPa and 100 kPa (with corresponding uncertainty of $\pm 1.7\%$ for P_{CO_2}), and $\pm 0.5\%$ for P_{total} ranging between 101 kPa and 600 kPa (with corresponding uncertainty of $\pm 1.5\%$ for P_{CO_2}).

(H₂O–DEEA–CO₂, H₂O–MAPA–CO₂, and H₂O–DEEA–MAPA–CO₂) at different amine concentrations as a function of CO₂ loading in the temperature ranging from 40 °C to 120 °C. The experimental method described in this work was first validated by carrying out measurements with 30 mass % MEA solutions and comparing it with the literature data at three different temperatures 40 °C, 80 °C, and 120 °C. For 30 mass % MEA solutions, the measured total pressures and the calculated CO₂ partial pressures as a function of CO₂ loading are tabulated in Table 1. These results are also presented graphically in Figure 4, which illustrates a good agreement between the data in this work and the literature data^{28–32,34,35} in the whole temperature range of 40 °C to 120 °C.

H₂O–DEEA–CO₂ System. For DEEA, the equilibrium total pressures were measured in 5 M ($\sim 61.1 \text{ mass \%}$) DEEA solutions as a function of CO₂ loading in the temperature range 40 °C to 120 °C. The results are presented in Table 2. Total pressure data measured in this work as a function of CO₂ loading were compared with the data from Monteiro et al.,³⁹ as shown in Figure 5. The two sets of data are in good agreement. The data measured in this work have good repeatability with a little scatter at 40 °C at high CO₂ loadings. The estimated CO₂

partial pressure data from this work and Monteiro et al.³⁹ are also compared and presented graphically in Figure 6. Again, a very good agreement between two sets of data can be observed.

It should be noted that the isotherm at 40 °C shows a high CO₂ loading capacity at relatively low CO₂ partial pressures. However, the CO₂ loading capacity of 5 M DEEA at 120 °C is very low and gives high CO₂ partial pressures. The cyclic capacity obtained from the difference in CO₂ loading between 40 °C (rich loading) and 120 °C (lean loading) is large. Therefore, DEEA with its high cyclic capacity and low heat of absorption³⁷ can be an attractive candidate for the energy efficient CO₂ absorbent. However, DEEA (a tertiary alkanol-amine) has low reaction kinetics which can lead to a very large size of the absorber.

H₂O–MAPA–CO₂ Systems. The equilibrium total pressure measurements were performed for two different concentrations, 2 M ($\sim 17.9 \text{ mass \%}$) and 1 M ($\sim 8.9 \text{ mass \%}$), of aqueous MAPA solutions as a function of CO₂ loading at three different temperatures 40 °C, 80 °C, and 120 °C. The results for 2 and 1 M MAPA solutions are respectively given in Tables 3 and 4. Both total pressure (right ordinate) and CO₂ partial pressure (left ordinate) data as a function of CO₂ loading are presented graphically in

Table 5. Total Pressure and Solubility of CO₂ in 5 M (63.533 mass %) DEEA + 2 M (19.116 mass %) MAPA Solutions ($b_{\text{mixture}} = 43.743 \text{ mol Amine} \cdot (\text{kg H}_2\text{O})^{-1}$) at 40 °C, 80 °C, and 120 °C^a

α_{CO_2}	b_{CO_2}	P_{total}	P_{CO_2}	α_{CO_2}	b_{CO_2}	P_{total}	P_{CO_2}	α_{CO_2}	b_{CO_2}	P_{total}	P_{CO_2}
$\text{mol CO}_2 \cdot (\text{mol amine})^{-1}$	$\text{mol CO}_2 \cdot (\text{kg H}_2\text{O})^{-1}$	kPa	kPa	$\text{mol CO}_2 \cdot (\text{mol amine})^{-1}$	$\text{mol CO}_2 \cdot (\text{kg H}_2\text{O})^{-1}$	kPa	kPa	$\text{mol CO}_2 \cdot (\text{mol amine})^{-1}$	$\text{mol CO}_2 \cdot (\text{kg H}_2\text{O})^{-1}$	kPa	kPa
313.15 K (1)				353.15 K (1)				393.15 K (1)			
0.335	14.651	16.1	5.0	0.199	8.695	42.5	0.9	0.027	1.160	170.5	2.9
0.385	16.821	29.0	17.9	0.243	10.633	46.3	4.7	0.066	2.872	177.8	10.2
0.434	18.973	47.2	36.1	0.286	12.517	62.6	21.0	0.108	4.709	190.3	22.7
0.481	21.025	68.2	57.1	0.327	14.311	126.0	84.4	0.152	6.638	205.7	38.1
0.527	23.032	92.5	81.4	0.372	16.285	265.6	224.0	0.189	8.282	229.5	61.9
0.565	24.720	116.9	105.8	0.408	17.859	417.2	375.6	0.228	9.963	278.5	110.9
0.595	26.042	139.2	128.1	0.432	18.904	527.7	486.1	0.264	11.560	376.2	208.6
0.620	27.121	157.7	146.6	0.439	19.199	556.6	515.0	0.299	13.085	552.4	384.8
0.642	28.084	177.5	166.4		353.15 K (2)			0.306	13.395	589.2	421.6
0.666	29.132	199.0	187.9	0.204	8.929	42.9	1.2		393.15 K (2)		
0.689	30.135	221.4	210.3	0.247	10.794	46.9	5.2	0.030	1.325	171.3	3.4
0.712	31.136	246.0	234.9	0.288	12.611	64.9	23.2	0.057	2.486	176.3	8.4
0.729	31.878	265.6	254.5	0.328	14.364	132.1	90.4	0.087	3.788	183.9	16.0
	313.15 K (2)			0.368	16.097	251.4	209.7	0.115	5.047	193.8	25.9
0.304	13.314	11.2	1.6	0.406	17.760	403.5	361.8	0.145	6.322	203.1	35.2
0.359	15.715	21.5	11.9	0.427	18.680	499.3	457.6	0.175	7.646	217.2	49.3
0.416	18.201	40.8	31.2	0.437	19.112	543.1	501.4	0.206	9.012	242.5	74.6
0.470	20.566	64.4	54.8					0.235	10.285	283.5	115.6
0.522	22.835	91.2	81.6					0.264	11.557	354.1	186.2
0.570	24.922	121.9	112.3					0.291	12.732	465.7	297.8
0.609	26.650	154.1	144.5					0.307	13.441	559.5	391.6
0.637	27.879	177.4	167.8					0.312	13.643	584.5	416.6
0.668	29.240	206.0	196.4								
0.695	30.411	233.7	224.1								
0.720	31.500	261.0	251.4								
0.743	32.496	288.1	278.5								

^aThe standard uncertainty for the temperature is $u(T) = 0.03 \text{ K}$, and the relative standard uncertainties for the CO₂ composition are $u_r(b) = 0.01$ and $u_r(\alpha) = 0.01$. The estimated uncertainty for the measured P_{total} is $\pm 1\%$ for the total pressure below 50 kPa (with corresponding uncertainty of $\pm 2\%$ for the calculated P_{CO_2}), $\pm 0.7\%$ for P_{total} ranging between 51 kPa and 100 kPa (with corresponding uncertainty of $\pm 1.7\%$ for P_{CO_2}), and $\pm 0.5\%$ for P_{total} ranging between 101 kPa and 600 kPa (with corresponding uncertainty of $\pm 1.5\%$ for P_{CO_2}).

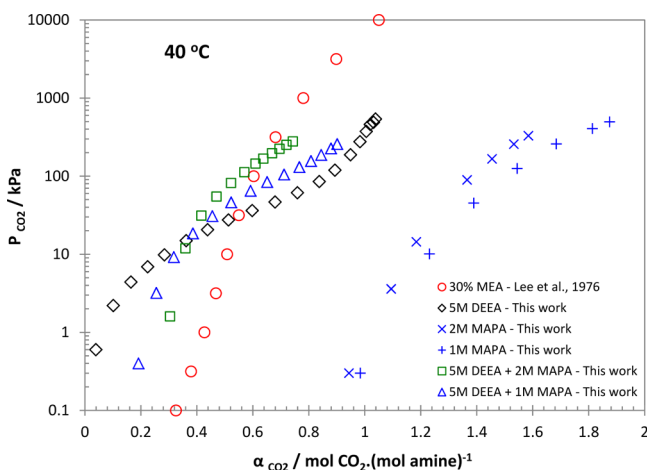


Figure 11. Comparison of CO₂ partial pressures as a function of loading for all the solvent systems studied in this work against the results of 30 mass % MEA at 40 °C.

Figure 7 for 2 M MAPA and Figure 8 for 1 M MAPA solutions. A good reproducibility can be observed in the data for both systems.

MAPA, being a diamine, shows a very high CO₂ loading capacity for both tested concentrations (2 and 1 M) at 40 °C. It also gives high CO₂ loading capacity at 120 °C, which results in

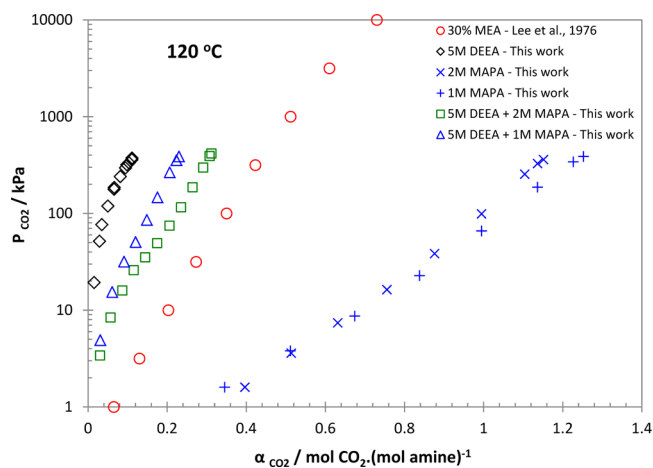


Figure 12. Comparison of CO₂ partial pressures as a function of loading for all the solvent systems studied in this work against the results of 30 mass % MEA at 120 °C.

relatively low cyclic capacity for MAPA compared to that of DEEA. MAPA has high heats of absorption³⁷ and this can lead to high regeneration energy requirements. However, the fast reaction kinetics of MAPA can lead to a reasonable size of the absorber.

Table 6. Total Pressure and Solubility of CO₂ in 5 M (62.025 mass %) DEEA + 1 M (9.331 mass %) MAPA Solutions ($b_{\text{mixture}} = 22.173 \text{ mol Amine} \cdot (\text{kg H}_2\text{O})^{-1}$) at 40 °C, 80 °C, and 120 °C^a

α_{CO_2}	b_{CO_2}	P_{total}	P_{CO_2}	α_{CO_2}	b_{CO_2}	P_{total}	P_{CO_2}	α_{CO_2}	b_{CO_2}	P_{total}	P_{CO_2}
$\frac{\text{mol CO}_2}{(\text{mol amine})^{-1}}$	$\frac{\text{mol CO}_2}{(\text{kg H}_2\text{O})^{-1}}$	kPa	kPa	$\frac{\text{mol CO}_2}{(\text{mol amine})^{-1}}$	$\frac{\text{mol CO}_2}{(\text{kg H}_2\text{O})^{-1}}$	kPa	kPa	$\frac{\text{mol CO}_2}{(\text{mol amine})^{-1}}$	$\frac{\text{mol CO}_2}{(\text{kg H}_2\text{O})^{-1}}$	kPa	kPa
313.15 K (1)				353.15 K (1)				393.15 K (1)			
0.223	4.943	13.2	1.4	0.137	3.027	50.7	3.7	0.031	0.684	200.1	4.9
0.271	6.016	16.3	4.5	0.187	4.148	63.3	16.3	0.061	1.349	210.6	15.4
0.320	7.086	21.6	9.8	0.234	5.192	99.6	52.6	0.091	2.016	227.0	31.8
0.374	8.300	29.2	17.4	0.279	6.190	158.7	111.7	0.120	2.665	245.8	50.6
0.427	9.472	38.4	26.6	0.320	7.105	230.0	183.0	0.149	3.294	280.9	85.7
0.481	10.672	49.7	37.9	0.366	8.120	323.4	276.4	0.175	3.889	342.0	146.8
0.531	11.770	61.7	49.9	0.407	9.026	423.0	376.0	0.206	4.574	461.1	265.9
0.579	12.840	74.9	63.1	0.435	9.634	496.8	449.8	0.223	4.955	549.6	354.4
0.626	13.886	90.3	78.5	0.453	10.041	545.2	498.2	0.230	5.097	582.9	387.7
0.680	15.075	107.7	95.9	0.463	10.260	568.9	521.9	393.15 K (2)			
0.732	16.237	128.8	117.0	353.15 K (2)				0.030	0.663	199.7	5.3
0.765	16.963	145.2	133.4	0.133	2.957	49.8	3.2	0.062	1.370	211.4	17.0
0.795	17.635	163.3	151.5	0.184	4.087	60.8	14.2	0.096	2.126	230.4	36.0
0.825	18.298	186.2	174.4	0.227	5.043	91.2	44.6	0.128	2.835	256.1	61.7
0.852	18.896	211.6	199.8	0.274	6.071	148.3	101.7	0.163	3.604	315.8	121.4
0.873	19.366	235.9	224.1	0.321	7.127	229.6	183.0	0.195	4.324	425.7	231.3
313.15 K (2)				0.364	8.064	314.7	268.1	0.220	4.878	552.3	357.9
0.191	4.245	9.6	0.4	0.405	8.972	411.4	364.8	0.227	5.034	582.3	387.9
0.255	5.658	12.4	3.2	0.438	9.716	501.3	454.7				
0.318	7.043	18.4	9.2	0.457	10.130	550.9	504.3				
0.386	8.559	27.7	18.5								
0.455	10.090	40.0	30.8								
0.522	11.584	55.3	46.1								
0.592	13.122	74.0	64.8								
0.651	14.432	93.3	84.1								
0.711	15.773	114.1	104.9								
0.766	16.985	139.7	130.5								
0.808	17.909	165.3	156.1								
0.844	18.720	195.7	186.5								
0.879	19.498	235.7	226.5								
0.901	19.984	266.9	257.7								

^aThe standard uncertainty for the temperature is $u(T) = 0.03 \text{ K}$, and the relative standard uncertainties for the CO₂ composition are $u_r(b) = 0.01$ and $u_r(\alpha) = 0.01$. The estimated uncertainty for the measured P_{total} is $\pm 1\%$ for the total pressure below 50 kPa (with corresponding uncertainty of $\pm 2\%$ for the calculated P_{CO_2}), $\pm 0.7\%$ for P_{total} ranging between 51 kPa and 100 kPa (with corresponding uncertainty of $\pm 1.7\%$ for P_{CO_2}), and $\pm 0.5\%$ for P_{total} ranging between 101 kPa and 600 kPa (with corresponding uncertainty of $\pm 1.5\%$ for P_{CO_2}).

H₂O–DEEA–MAPA–CO₂ Systems. In this study, two aqueous DEEA–MAPA mixtures, 5 M (~ 63.5 mass %) DEEA + 2 M (19.1 mass %) MAPA and 5 M (~ 62 mass %) DEEA + 1 M (~ 9.3 mass %) MAPA, were examined in the temperature range 40 °C to 120 °C. These mixtures, 5 M DEEA + 2 M MAPA and 5 M DEEA + 1 M MAPA, are respectively abbreviated as 5D2M and 5D1M. Both mixtures gave two liquid phases in a certain CO₂ loading range. The measured equilibrium total pressure and the estimated CO₂ partial pressure data in 5D2M and 5D1M are presented respectively in Tables 5 and 6. The total pressure (right ordinate) and the CO₂ partial pressure (left ordinate) data as a function of CO₂ loading are also presented graphically in Figures 9 and 10 for 5D2M and 5D1M, respectively.

MAPA (fast reaction kinetics), having primary and secondary amine functional groups, is expected to react first in the aqueous amine mixtures compared to that of DEEA (slow reaction kinetics), a tertiary alkanolamine. This can be observed in the results of CO₂ partial pressures against loading at 40 °C in Figure 9 for 5D2M. The isotherm is quite steep up to a certain CO₂ loading ($\sim 0.45 \text{ mol CO}_2 \cdot (\text{mol amine})^{-1}$),

showing a qualitative behavior similar to that of H₂O–MAPA–CO₂ systems, and then the slope of the line decreases, which shows a qualitative behavior similar to that of the H₂O–DEEA–CO₂ system. Such a trend can also be seen for 5D1M at 40 °C in Figure 10. However, MAPA seems to be the dominating reacting component (with CO₂) in both amine mixtures at high temperatures, which can be observed from the steepness of the isotherms. This may be due to the reduced absorption capacity of DEEA at high temperatures, e.g., the isotherm at 120 °C in Figure 6. Both tested aqueous amine mixtures, 5D2M and 5D1M, gave liquid–liquid phase split in a certain CO₂ loading range. A detail description on the phase change behavior of these amine mixtures can be found in our previous work.³⁷

A comparison of CO₂ partial pressures as a function of loading for all the solvent systems studied in this work with 30 mass % MEA is given in Figure 11 for 40 °C and Figure 12 for 120 °C. Both 2 and 1 M MAPA (diamine) solutions have shown very high CO₂ loading capacities at 40 °C and 120 °C compared to the results of 30 mass % MEA. The 5 M DEEA

isotherms, on the other hand, show a very different behavior at 40 °C and also gave high CO₂ partial pressures at low loadings at 120 °C compared to the results of 30 mass % MEA. These kinds of isotherms of DEEA at 40 °C and 120 °C result in high equilibrium temperature sensitivity, which can lead to the lower stripping steam requirements for solvent regeneration compared to the results of 30 mass % MEA. Another advantage is the possibility of solvent regeneration at elevated pressures leading to high pressure CO₂ streams at the top of the desorber. This can reduce the cost of CO₂ compression during transportation to the storage site. The aqueous mixtures, 5D2M and 5D1M, show a kind of results similar to that of 5 M DEEA at 40 °C and 120 °C depending on the concentration of the promoter (MAPA). Heats of absorption of CO₂ in these mixtures are relatively lower than 30 mass % MEA.³⁷

The differential enthalpy of absorption of CO₂ in aqueous amine solutions at constant CO₂ loading can be estimated from the equilibrium CO₂ solubility data by using following form of the Gibbs–Helmholtz equation.⁴⁰

$$\frac{\Delta H_{\text{abs}}}{R} = \left(\frac{\partial \ln P_{\text{CO}_2}}{\partial (1/T)} \right)_x \quad (1)$$

where ΔH_{abs} is the enthalpy of absorption, R is the gas constant, P_{CO_2} is the equilibrium CO₂ partial pressure, T is the temperature, and x is the equilibrium CO₂ loading.

On the basis of eq 1, the enthalpies of absorption were estimated at constant CO₂ loading from the slope of the linear plot between $\ln P_{\text{CO}_2}$ and $1/T$. The estimated enthalpies of absorption are 62.8 kJ·(mol CO₂)⁻¹, 84 kJ·(mol CO₂)⁻¹, 83.6 kJ·(mol CO₂)⁻¹, 70.1 kJ·(mol CO₂)⁻¹, and 69.7 kJ·(mol CO₂)⁻¹ for 5 M DEEA, 2 M MAPA, 1 M MAPA, 5D2M, and 5D1M, respectively, at constant CO₂ loadings of 0.1, 0.8, 0.72, 0.31, and 0.25 mol CO₂·(mol amine)⁻¹. These estimated values of enthalpy of absorption are almost similar to the values measured calorimetrically at 40 °C in our previous work at respective CO₂ loadings.³⁷ However, these values are significantly different from the values measured at 80 °C and 120 °C.

4. CONCLUSIONS

Equilibrium total pressures were measured and equilibrium CO₂ partial pressures were estimated from the total pressure measurements as a function of CO₂ loading in binary and ternary aqueous solutions of 2-(diethylamino)ethanol (DEEA) and 3-(methylamino)propylamine (MAPA). The measurements were performed isothermally in a reaction calorimeter used as an equilibrium cell. The tested systems were the binary aqueous solutions of 5 M DEEA, 2 M MAPA, and 1 M MAPA, and the ternary aqueous mixtures of 5 M DEEA + 2 M MAPA and 5 M DEEA + 1 M MAPA. The selected compositions of aqueous amine mixtures gave liquid–liquid phase split upon CO₂ absorption. The total pressures were measured, and the CO₂ partial pressures were calculated as a function of CO₂ loading at three different temperatures 40 °C, 80 °C, and 120 °C. All experiments were reproduced with a good repeatability.

Measurements were also carried out in 30 mass % MEA solutions and compared with the literature data to validate the experimental method used in this work. All the measured data were compared with the results of 30 mass % MEA as a reference case. 5 M DEEA has shown high cyclic capacity. Both 2 and 1 M MAPA showed high loading capacities at 40 °C and 120 °C. The aqueous amine blends, 5D2M and 5D1M, gave

fairly good cyclic capacities and their results depend on concentration of the promoter (MAPA) in the amine blend. Due to high CO₂ partial pressure at low loadings, the studied mixtures can also allow the stripping process at elevated desorber pressures, thereby reducing the energy requirements for the CO₂ compression. Approximate enthalpies of absorption of CO₂ in all the tested aqueous amine systems were estimated from the CO₂ solubility data. The measured total pressure and the estimated CO₂ solubility data can be useful in thermodynamic modeling of the capture systems when aqueous DEEA–MAPA solutions are used as capture solvents.

■ AUTHOR INFORMATION

Corresponding Author

*K. Thomsen: tel, +45 4525 2860; fax, +45 4588 2258; e-mail address, kth@kt.dtu.dk.

Funding

We greatly acknowledge the financial support from European Commission under the seventh Framework Program (Grant Agreement No. 241393) through the iCap project.

Notes

The authors declare no competing financial interest.

■ ACKNOWLEDGMENTS

Inna Kim and Anastasia Trollebo are acknowledged for the technical support.

■ REFERENCES

- (1) Metz, B.; Davidson, O.; Bosch, P.; Dave, R.; Meyer, L., Eds. *Climate Change 2007 – Mitigation of Climate Change*; Working Group III Contribution to the Fourth Assessment Report of the Intergovernmental Panel on Climate Change; Cambridge University Press: Oxford, U.K., 2007.
- (2) Adams, D.; Davison, J. *Capturing CO₂*. IEA Greenhouse Gas R&D Programme, 2007.
- (3) Metz, B.; Davidson, O.; de Coninck, H.; Loos, M.; Meyer, L., Eds. *Carbon Dioxide Capture and Storage*; Intergovernmental Panel on Climate Change (IPCC); Cambridge University Press: Oxford, U.K., 2005.
- (4) *The Global Status of CCS: 2012*; Global CCS Institute: Canberra, Australia, 2012.
- (5) Kohl, A. L.; Nielsen, R. B. *Gas Purification*, 5th ed.; Gulf Publishing Co.: Houston, TX, USA, 1997.
- (6) Zhao, M.; Minett, A. I.; Harris, A. T. A review of techno-economic models for the retrofitting of conventional pulverised-coal power plants for post-combustion capture (PCC) of CO₂. *Energy Environ. Sci.* **2013**, *6*, 25–40.
- (7) Dillon, D.; Wheeldon, J.; Chu, R.; Choi, G.; Loy, C. A Summary of EPRI's Engineering and Economic Studies of Post Combustion Capture Retrofit Applied at Various North American Host Sites. *Energy Procedia* **2013**, *37*, 2349–2358.
- (8) Davidson, R. M. *Post-combustion Carbon Capture from Coal Fired Plants - Solvent Scrubbing*; IEA Clean Coal Centre: London, 2007; CCC/125.
- (9) Wang, M.; Lawal, A.; Stephenson, P.; Sidders, J.; Ramshaw, C. Post-combustion CO₂ capture with chemical absorption: A state-of-the-art review. *Chem. Eng. Res. Des.* **2011**, *89*, 1609–1624.
- (10) Glasscock, D. A.; Critchfield, J. E.; Rochelle, G. T. CO₂ absorption/desorption in mixtures of methyl-diethanolamine with monoethanolamine or diethanolamine. *Chem. Eng. Sci.* **1991**, *46* (11), 2829–2845.
- (11) Bougie, F.; Iliuta, M. C. Sterically Hindered Amine-Based Absorbents for the Removal of CO₂ from Gas Streams. *J. Chem. Eng. Data* **2012**, *57*, 635–669.

- (12) Rochelle, G. T.; Chen, E.; Freeman, S.; Wagener, D. V.; Xu, Q.; Voice, A. Aqueous piperazine as the new standard for CO₂ capture technology. *Chem. Eng. J.* **2011**, *171*, 725–733.
- (13) Mehdizadeh, H.; Gupta, M.; Kim, I.; Da Silva, E. F.; Haug-Warberg, T.; Svendsen, H. F. AMP-CO₂-water thermodynamics, a combination of UNIQUAC model, computational chemistry and experimental data. *Int. J. Greenhouse Gas Control* **2013**, *18*, 173–182.
- (14) Le Tourneux, D.; Iliuta, I.; Iliuta, M. C.; Fradette, S.; Larachi, F. Solubility of carbon dioxide in aqueous solutions of 2-amino-2-hydroxymethyl-1,3-propanediol. *Fluid Phase Equilib.* **2008**, *268*, 121–129.
- (15) Bougie, F.; Iliuta, M. C. CO₂ Absorption in Aqueous Piperazine Solutions: Experimental Study and Modeling. *J. Chem. Eng. Data* **2011**, *56*, 1547–1554.
- (16) Bröder, P.; Grimstedt, A.; Mejdell, T.; Svendsen, H. F. CO₂ capture into aqueous solutions of piperazine activated 2-amino-2-methyl-1-propanol. *Chem. Eng. Sci.* **2011**, *66*, 6193–6198.
- (17) Fosbøl, P. L.; Neerup, R.; Arshad, M. W.; Teclé, Z.; Thomsen, K. Aqueous Solubility of Piperazine and 2-Amino-2-methyl-1-propanol plus Their Mixtures Using an Improved Freezing-Point Depression Method. *J. Chem. Eng. Data* **2011**, *56*, 5088–5093.
- (18) Bougie, F.; Iliuta, M. C. CO₂ Absorption into Mixed Aqueous Solutions of 2-Amino-2-hydroxymethyl-1,3-propanediol and Piperazine. *Ind. Eng. Chem. Res.* **2010**, *49*, 1150–1159.
- (19) Zhu, D.; Fang, M.; Lv, Z.; Wang, Z.; Luo, Z. Selection of Blended Solvents for CO₂ Absorption from Coal-Fired Flue Gas. Part I: Monoethanolamine (MEA)-Based Solvents. *Energy Fuels* **2012**, *26*, 147–153.
- (20) Adeosun, A.; Abu-Zahra, M. R. M. Evaluation of amine-blend solvent systems for CO₂ post-combustion capture applications. *Energy Procedia* **2013**, *37*, 211–218.
- (21) Dubois, L.; Thomas, D. Postcombustion CO₂ capture by chemical absorption: screening of aqueous amine(s)-based solvents. *Energy Procedia* **2013**, *37*, 1648–1657.
- (22) Svendsen, H. F.; Hessen, E. T.; Mejdell, T. Carbon dioxide capture by absorption, challenges and possibilities. *Chem. Eng. J.* **2011**, *171*, 718–724.
- (23) Zhang, J.; Nwani, O.; Tan, Y.; Agar, D. W. Carbon dioxide absorption into biphasic amine solvent with solvent loss reduction. *Chem. Eng. Res. Des.* **2011**, *89*, 1190–1196.
- (24) Raynal, L.; Pascal, A.; Bouillon, P.-A.; Gomez, A.; le Febvre de Nailly, M.; Jacquin, M.; Kittel, J.; di Lella, A.; Mougin, P.; Trapy, J. The DMXTM process: an original solution for lowering the cost of post-combustion carbon capture. *Energy Procedia* **2011**, *4*, 779–786.
- (25) Raynal, L.; Bouillon, P.-A.; Gomez, A.; Broutin, P. From MEA to demixing solvents and future steps, a roadmap for lowering the cost of post-combustion carbon capture. *Chem. Eng. J.* **2011**, *171*, 742–752.
- (26) Zhang, J.; Misch, R.; Tan, Y.; Agar, D. W. Novel thermomorphic biphasic amine solvents for CO₂ absorption and low-temperature extractive regeneration. *Chem. Eng. Technol.* **2011**, *34* (9), 1481–1489.
- (27) Zhang, J.; Agar, D. W.; Zhang, X.; Geuzebroek, F. CO₂ absorption in biphasic solvents with enhanced low temperature solvent regeneration. *Energy Procedia* **2011**, *4*, 67–74.
- (28) Lee, J. I.; Otto, F. D.; Mather, A. E. Equilibrium Between Carbon Dioxide and Aqueous Monoethanolamine Solutions. *J. Appl. Chem. Biotechnol.* **1976**, *26*, 541–549.
- (29) Shen, K.-P.; Li, M.-H. Solubility of Carbon Dioxide in Aqueous Mixtures of Monoethanolamine with Methyl-diethanolamine. *J. Chem. Eng. Data* **1992**, *37*, 96–100.
- (30) Jou, F.-Y.; Mather, A. E.; Otto, F. D. The Solubility of CO₂ in a 30 Mass Percent Monoethanolamine Solution. *Can. J. Chem. Eng.* **1995**, *73*, 140–147.
- (31) Ma'mun, S.; Nilsen, R.; Svendsen, H. F. Solubility of Carbon Dioxide in 30 mass % Monoethanolamine and 50 mass % Methyl-diethanolamine Solutions. *J. Chem. Eng. Data* **2005**, *50*, 630–634.
- (32) Aronu, U. E.; Gondal, S.; Hessen, E. T.; Haug-Warberg, T.; Hartono, A.; Hoff, K. A.; Svendsen, H. F. Solubility of CO₂ in 15, 30, 45 and 60 mass% MEA from 40 to 120 °C and model representation using the extended UNIQUAC framework. *Chem. Eng. Sci.* **2011**, *66*, 6393–6406.
- (33) Anufrikov, Y. A.; Kuranov, G. L.; Smirnova, N. A. Solubility of CO₂ and H₂S in Alkanolamine-containing Aqueous Solutions. *Russ. J. Appl. Chem.* **2007**, *80* (4), 515–527.
- (34) Xu, Q.; Rochelle, G. T. Total Pressure and CO₂ Solubility at High Temperature in Aqueous Amines. *Energy Procedia* **2011**, *4*, 117–124.
- (35) Xu, Q. Thermodynamics of CO₂ Loaded Aqueous Amines. *Ph.D. Thesis*, The University of Texas at Austin, Austin, TX, 2011.
- (36) Arshad, M. W.; von Solms, N.; Svendsen, H. F.; Thomsen, K. Heat of Absorption of CO₂ in Aqueous Solutions of DEEA, MAPA and their Mixture. *Energy Procedia* **2013**, *37*, 1532–1542.
- (37) Arshad, M. W.; Fosbøl, P. L.; von Solms, N.; Svendsen, H. F.; Thomsen, K. Heat of Absorption of CO₂ in Phase Change Solvents: 2-(diethylamino)ethanol and 3-(methylamino)propylamine. *J. Chem. Eng. Data* **2013**, *58*, 1974–1988.
- (38) Kim, I.; Svendsen, H. F. Heat of absorption of carbon dioxide (CO₂) in monoethanolamine (MEA) and 2-(aminoethyl)-ethanolamine (AEEA) solutions. *Ind. Eng. Chem. Res.* **2007**, *46*, 5803–5809.
- (39) Monteiro, J. G. M.-S.; Pinto, D. D. D.; Zaidy, S. A. H.; Hartono, A.; Svendsen, H. F. VLE data and modelling of aqueous N,N-diethylethanolamine (DEEA) solutions. *Int. J. Greenhouse Gas Control* **2013**, *19*, 432–440.
- (40) Sherwood, A. E.; Prausnitz, J. M. The heat of solution of gases at high pressure. *AIChE J.* **1962**, *8* (4), 519–521.